Electronic Supplementary Material (ESI) for Journal of Materials Chemistry A.

Supplementary Information for

Design of Anode Functional Layers for Protonic Solid Oxide Electrolysis Cells

Chunmei Tang,[a] Ning Wang,[b] Ruijie Zhu,[a] Sho Kitano,[c] Hiroki Habazaki,[c] and Yoshitaka Aoki*[c]

[a] Graduate School of Chemical Sciences and Engineering, Hokkaido University, N13W8, Kita-ku, Sapporo, 060-8628, Japan.

[b] Huangpu Hydrogen Energy Innovation Center/Guangzhou Key Laboratory for Clean Energy and Materials, School of chemistry and Chemical Engineering, Guangzhou University, Guangzhou, 510006, China

[c] Faculty of Engineering, Hokkaido University, N13W8, Kita-ku, Sapporo, 060-8628, Japan.

E-mail: y-aoki@eng.hokudai.ac.jp

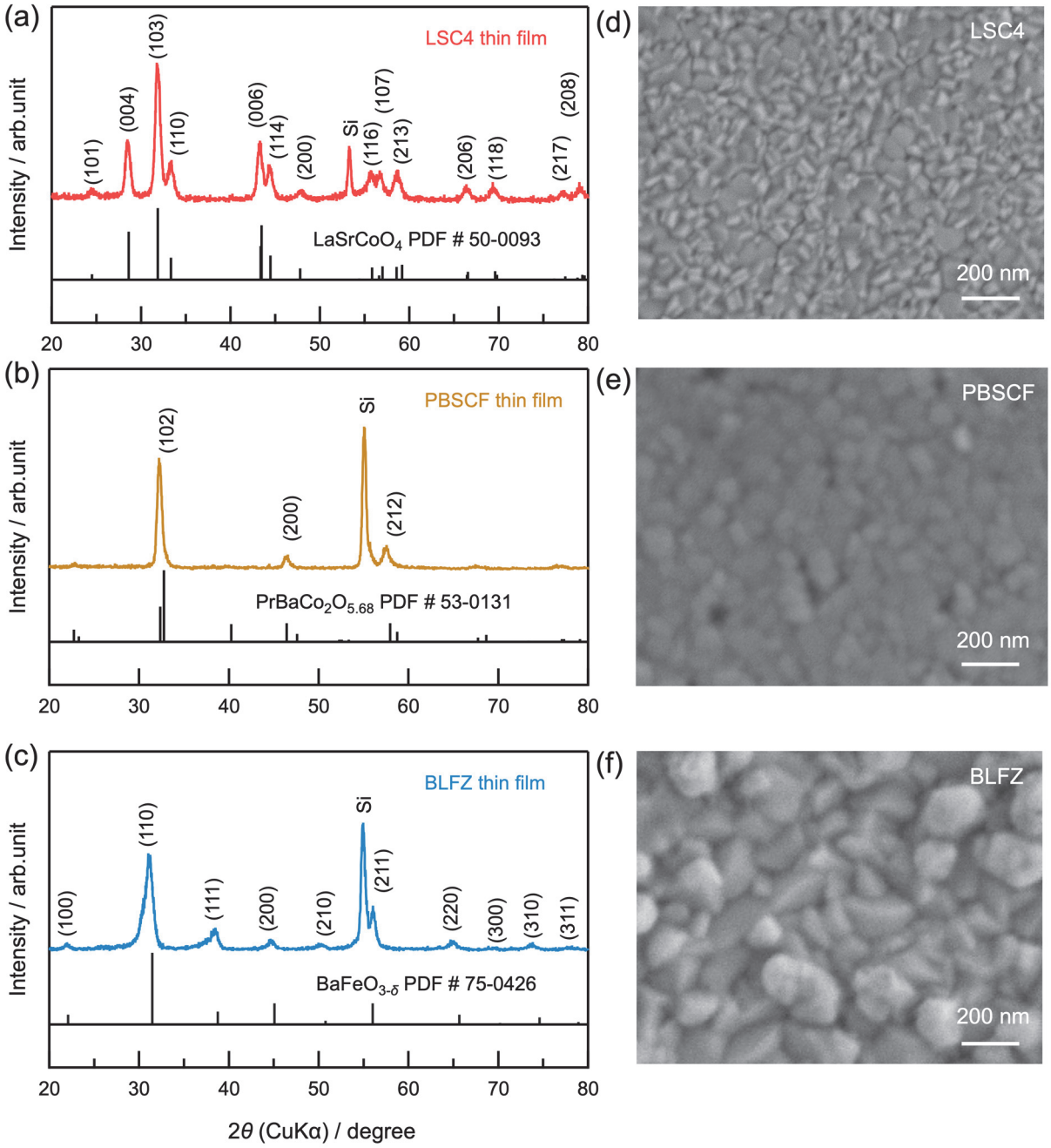

Fig. S1. GIXRD patterns and the surface SEM images of LSC4, PBSCF and BLFZ thin films deposited on a silicon wafer.

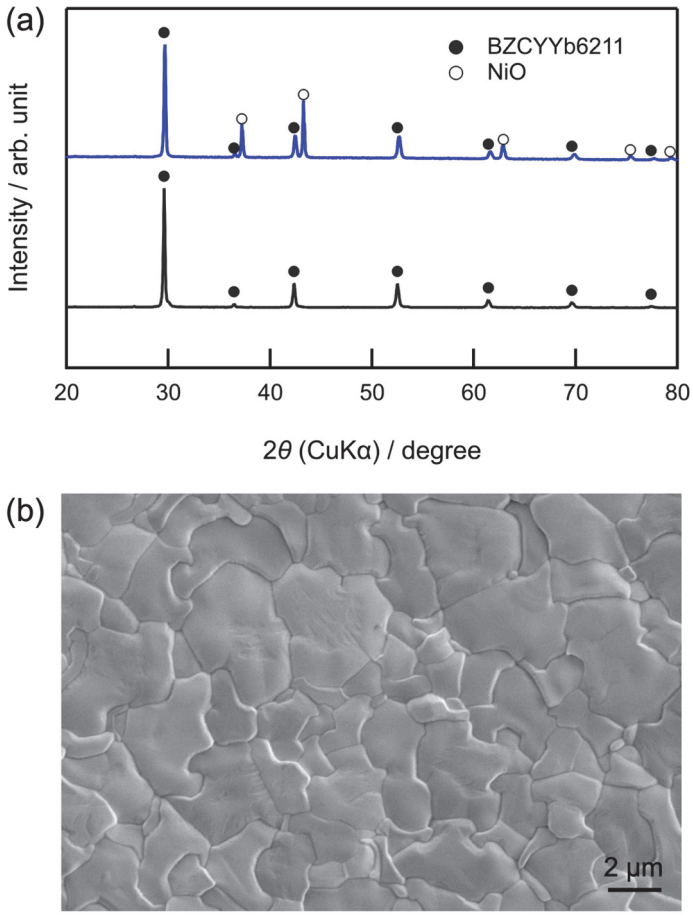

Fig. S2. XRD and surface SEM image of BZCYYb6211 based cell. (a) Powder XRD patterns of as synthesized BZCYYb6211 at 1300 °C for 10 h and BZCYYb6211-NiO composite bulk at 1450 °C for 8 h. (b) Surface SEM image of BZCYYb6211 electrolyte film.

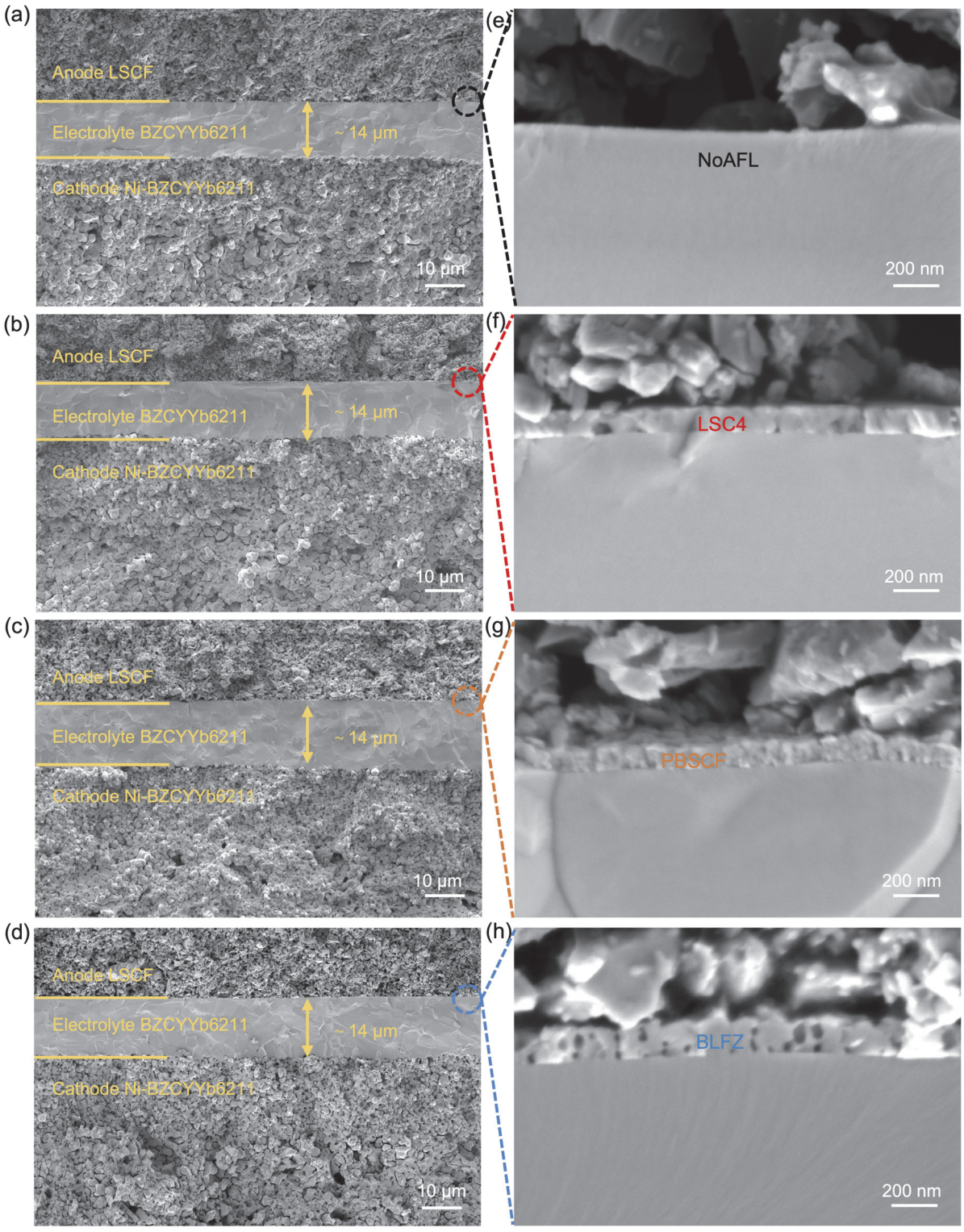

Fig. S3. Cross-sectional SEM images of Ni-BZCYYb6211 cathode-supported P-SOECs. (a) Cell without anode functional layer (NoAFL). (b)-(d) Cells with LSC4, PBSCF, and BLFZ AFL, respectively. (e)-(h) Corresponding enlarged SEM images of interfaces between LSCF anode and BZCYYb6211 electrolyte.

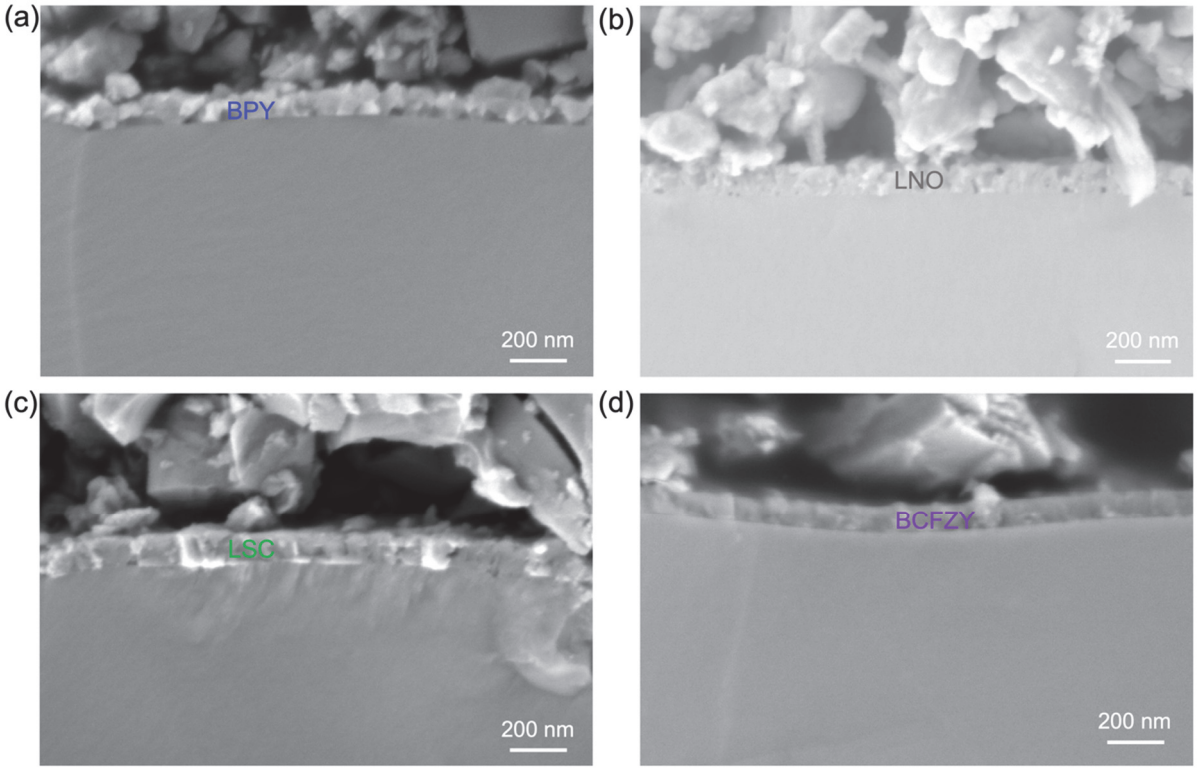

Fig. S4. Cross-sectional SEM images of the interfaces between LSCF anode and BZCYYb6211 electrolyte of various AFL cells. (a) BPY. (b) LNO. (c) LSC. (d) BCFZY.

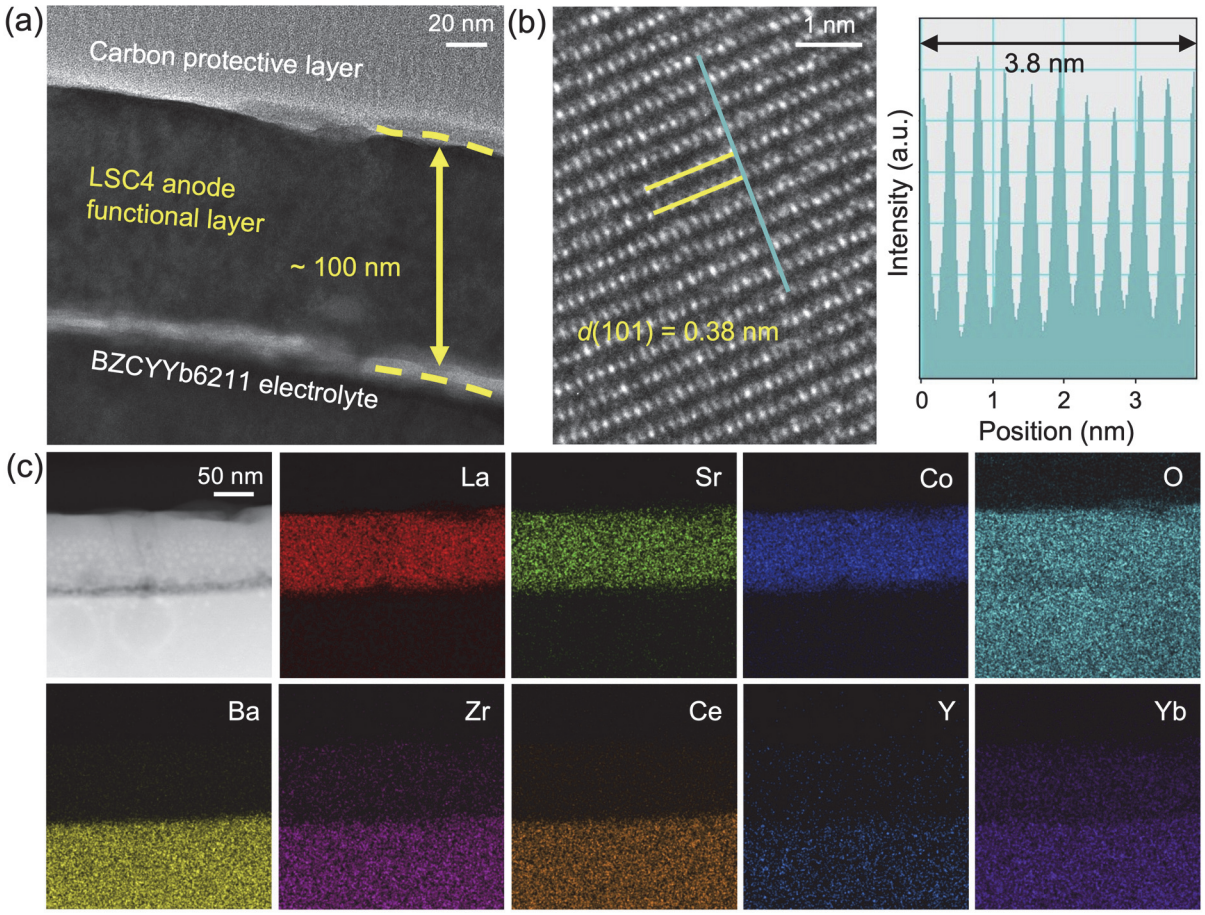

Fig. S5. High-resolution electron micrographs of LSC4 thin films. (a) Cross-sectional TEM image of interfaces between the LSC4 interlayer and BZCYYb6211 electrolyte. (b) Lattice fringes of LSC4 and corresponding line scan histogram along the blue line. (c) EDX element mapping of LSC4 thin film.

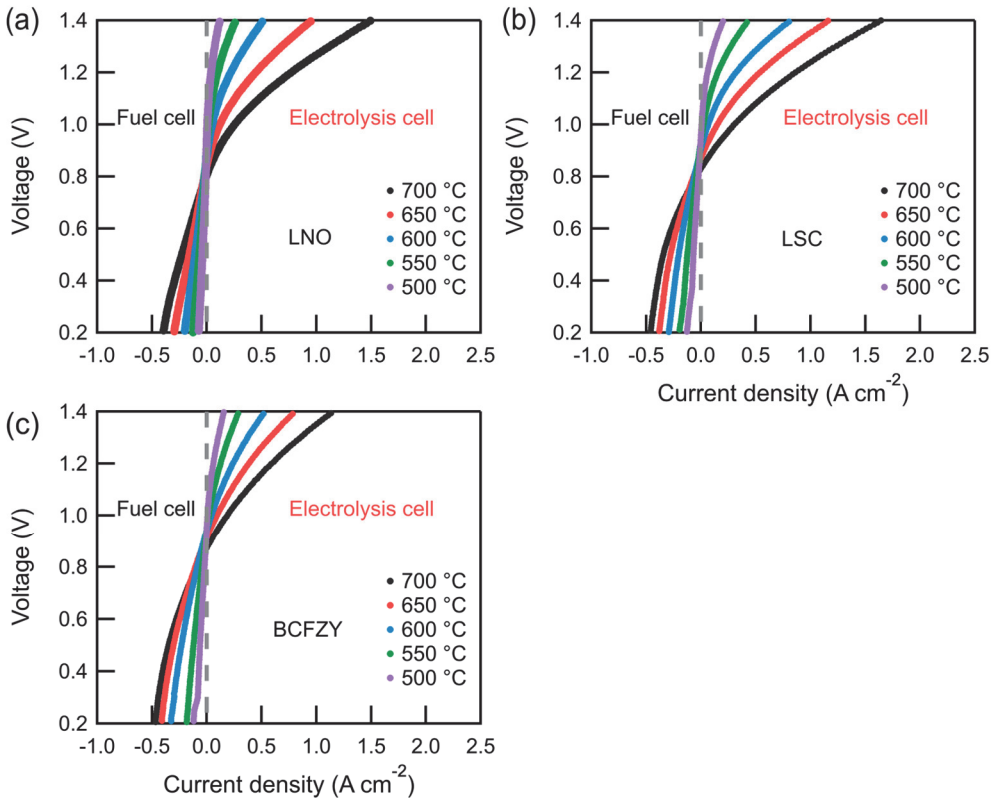

Fig. S6. Current–voltage (*I–V*) characteristics of various AFL cells. (a) LNO. (b) LSC. (c) BCFZY.

Table S1 Performances in P-SOECs with double conductor anode at 600 ℃ under 1.3 V in recent years.

Configuration of electrolysis cell: Anode/electrolyte (thickness)/cathode	Inlet gas composition Anode	Cathode	*I* ($A\ cm^{-2}$)	Ref.
SSC-BZCY352/BZCY352 (20 μm)/Ni-BZCY352	Air (50% H_2O)	100% H_2	~0.19	1
LSC-BZCYbCo/BZCYbCo (45 μm)/Ni-BZCYbCo	Air (30% H_2O)	10% H_2/He	0.03	2
LSCF-BZY82/BZY91 (15 μm)/Ni-BZY82	Air (3% H_2O)	4% H_2/Ar	0.05	3
LSCF/BZCY442 (24 μm)/Ni-BZCY442	Air (3% H_2O)	97% H_2 (3% H_2O)	0.50	4
LNO-BZCDy/ BZCDy (30 μm)/Ni-BZCDy	Air (90% H_2O)	97% H_2 (3% H_2O)	0.16	5
SFM-BZY82/BZY82 (16 μm)/Ni-BZY82	Air (3% H_2O)	10% H_2/N_2	0.21	6
SFM-BZY82/BZY82 (18 μm)/Ni-BZCY172	Air (3% H_2O)	20% H_2/N_2	0.38	7
SEFC-BZCY532/BZCY532 (15 μm)/Ni-BZCY532	Air (10% H_2O)	97% H_2 (3% H_2O)	0.42	4
SLF/BZCY352 (20 μm)/Ni-BZCY352	Air (20% H_2O)	97% H_2 (3% H_2O)	0.46	8
LSN/BZCY172 (15 μm)/Ni-BZCY172	Air (20% H_2O)	97% H_2 (3% H_2O)	0.42	9
LSN/BZCYYbCu (13 μm)/Ni-BZCYYbCu	Air (20% H_2O)	97% H_2 (3% H_2O)	0.59	10
PNO-BZCY262/ BZCY262 (20 μm)/ Ni-BZCY262	Air (40% H_2O)	100% H_2	0.60	11
PBSCF/BZCYYb (20 μm)/Ni-BZCYYb	O_2 (3% H_2O)	100% H_2	0.55	12
BCFZY-BZCY361/BZCYSm (25 μm)/Ni-BZCYSm	Air (12% H_2O)	97% H_2 (3% H_2O)	0.37	13
SCFN/BZCYYb1711 (26 μm)/Ni-BZCYYb1711	Air (3% H_2O)	100% H_2	0.36	14
LSCF/BZCYYb6211 (14 μm)/Ni-BZCYYb6211	Air (30% H_2O)	10% H_2/Ar (3% H_2O)	0.39	This work
LSCF/LSC4/BZCYYb6211 (14 μm)/Ni-BZCYYb6211	Air (30% H_2O)	10% H_2/Ar (3% H_2O)	0.73	This work
LSCF/PBSCF/BZCYYb6211 (14 μm)/Ni-BZCYYb6211	Air (30% H_2O)	10% H_2/Ar (3% H_2O)	0.65	This work
LSCF/BLFZ/BZCYYb6211 (14 μm)/Ni-BZCYYb6211	Air (30% H_2O)	10% H_2/Ar (3% H_2O)	0.57	This work

Abbreviations of anode: $Sm_{0.5}Sr_{0.5}CoO_{3-\delta}$ (SSC); $(LaSr)CoO_{3-\delta}$ (LSC); $La_{0.6}Sr_{0.4}Co_{0.2}Fe_{0.8}O_{3-\delta}$ (LSCF); $La_2NiO_{4+\delta}$ (LNO); $Sr_2Fe_{1.5}Mo_{0.5}O_{6-\delta}$ (SFM); $SrEu_2Fe_{1.8}Co_{0.2}O_{7-\delta}$ (SEFC); $Sr_{2.8}La_{0.2}Fe_2O_{7-\delta}$ (SLF); $La_{1.2}Sr_{0.8}NiO_4$ (LSN); $Pr_2NiO_{4+\delta}$ (PNO); $PrBa_{0.5}Sr_{0.5}Co_{2-x}Fe_xO_{5+\delta}$ (PBSCF); $BaCo_{0.4}Fe_{0.4}Zr_{0.1}Y_{0.1}O_{3-\delta}$ (BCFZY); $Sr_{0.9}Ce_{0.1}Fe_{0.8}Ni_{0.2}O_{3-\delta}$(SCFN).

Abbreviations of electrolyte and fuel electrode: $BaZr_{0.3}Ce_{0.5}Y_{0.2}O_{3-\delta}$ (BZCY352); $BaZr_{0.40}Ce_{0.48}Yb_{0.1}Co_{0.02}O_{3-\delta}$ (BZCYbCo); $BaZr_{0.8}Y_{0.2}O_{3-\delta}$ (BZY82); $BaZr_{0.9}Y_{0.1}O_{3-\delta}$ (BZY91); $BaZr_{0.4}Ce_{0.4}Y_{0.2}O_{3-\delta}$ (BZCY442); $BaZr_{0.3}Ce_{0.5}Dy_{0.2}O_{3-\delta}$ (BZCDy); $BaZr_{0.5}Ce_{0.3}Y_{0.2}O_{3-\delta}$ (BZCY532); $BaZr_{0.3}Ce_{0.5}Y_{0.2}O_{3-\delta}$ (BZCY352); $BaZr_{0.1}Ce_{0.7}Y_{0.2}O_{3-\delta}$ (BZCY172); $BaZr_{0.1}Ce_{0.68}Y_{0.1}Yb_{0.1}Cu_{0.02}O_{3-\delta}$ (BZCYYbCu); $BaZr_{0.2}Ce_{0.6}Y_{0.2}O_{3-\delta}$ (BZCY262); $BaZr_{0.1}Ce_{0.7}Y_{0.2-x}Yb_xO_{3-\delta}$ (BZCYYb); $BaZr_{0.3}Ce_{0.6}Y_{0.1}O_{3-\delta}$ (BZCY361); $BaZr_{0.1}Ce_{0.7}Y_{0.1}Yb_{0.1}O_{3-\delta}$ (BZCYYb1711); $BaZr_{0.6}Ce_{0.2}Y_{0.1}Yb_{0.1}O_{3-\delta}$ (BZCYYb6211).

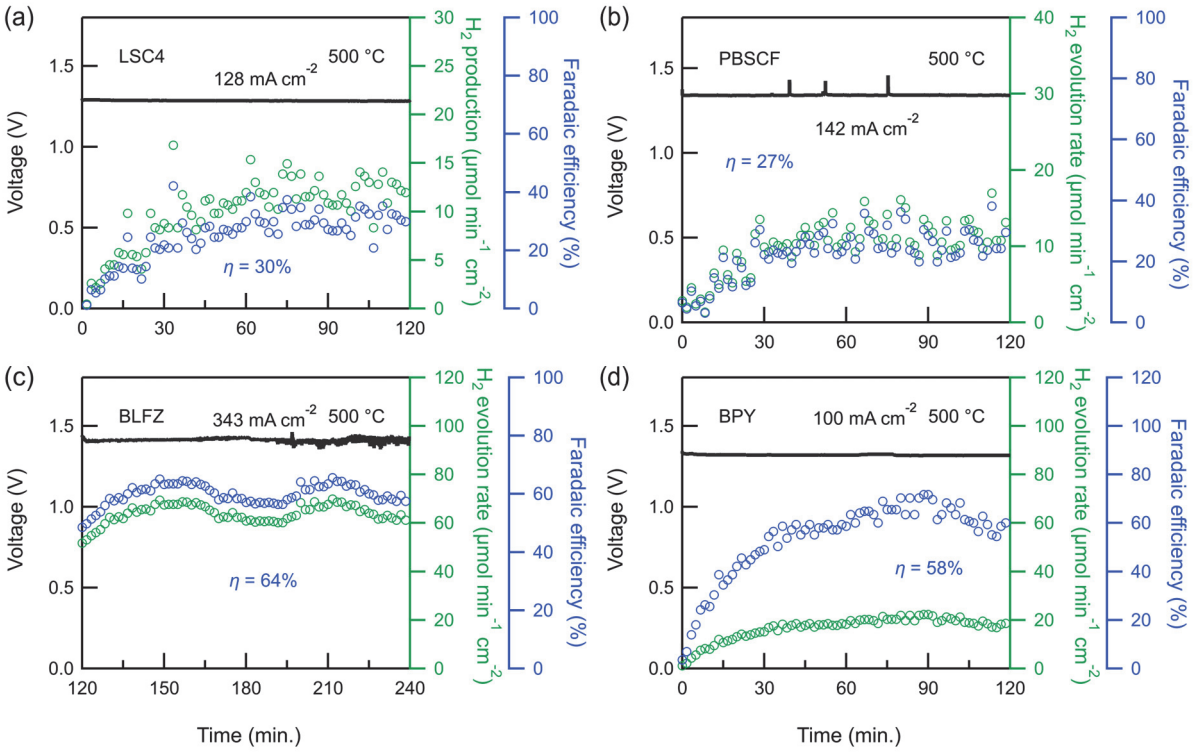

Fig. S7. Transients of cell voltages and H_2 gas evolution rates during galvanostatic electrolysis at 500 °C. (a) LSC4 AFL cell with applied current of 128 mA cm^{-2} at 1.3 V. (b) PBSCF AFL cell with applied current of 142 mA cm^{-2} at 1.3 V. (c) BLFZ AFL cell with applied current of 343 mA cm^{-2} at 1.4V. (d) BPY AFL cell with applied current of 100 mA cm^{-2} at 1.3 V.

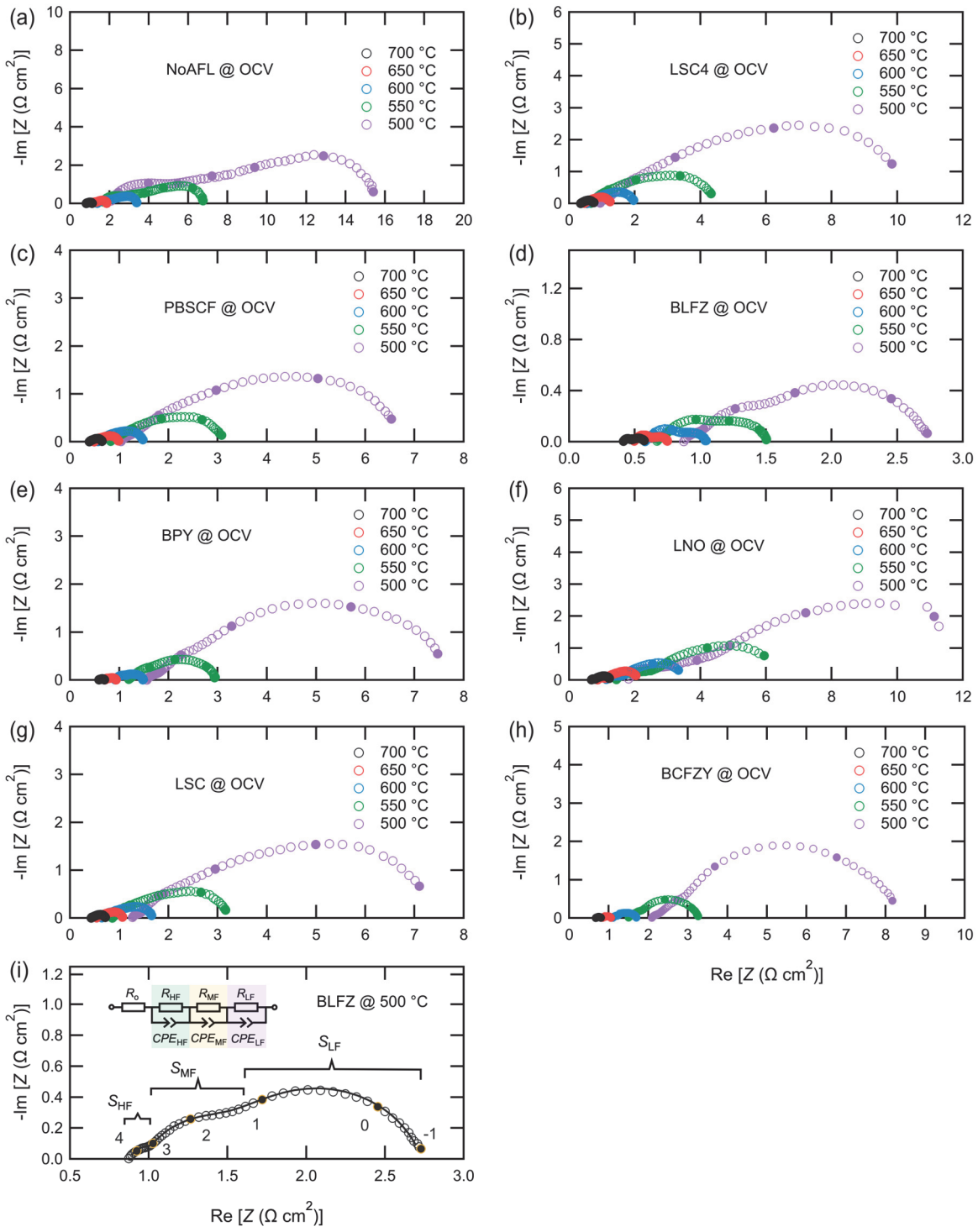

Fig. S8. Electrochemical impedance spectra (EIS) of P-SOECs with various AFLs ranging from 700 °C to 500 °C under OCV condition. (a) NoAFL. (b) LSC4. (c) PBSCF. (d) BLFZ. (e) BPY. (f) LNO. (g) LSC. (h) BCFZY. (i) EIS of BLFZ AFL cell at 500 °C, circles are observed data and solid line is fitting result with equivalent circuit model of R_o–(R_{HF}–CPE$_{HF}$)–(R_{MF}–CPE$_{MF}$)–(R_{LF}–CPE$_{LF}$)

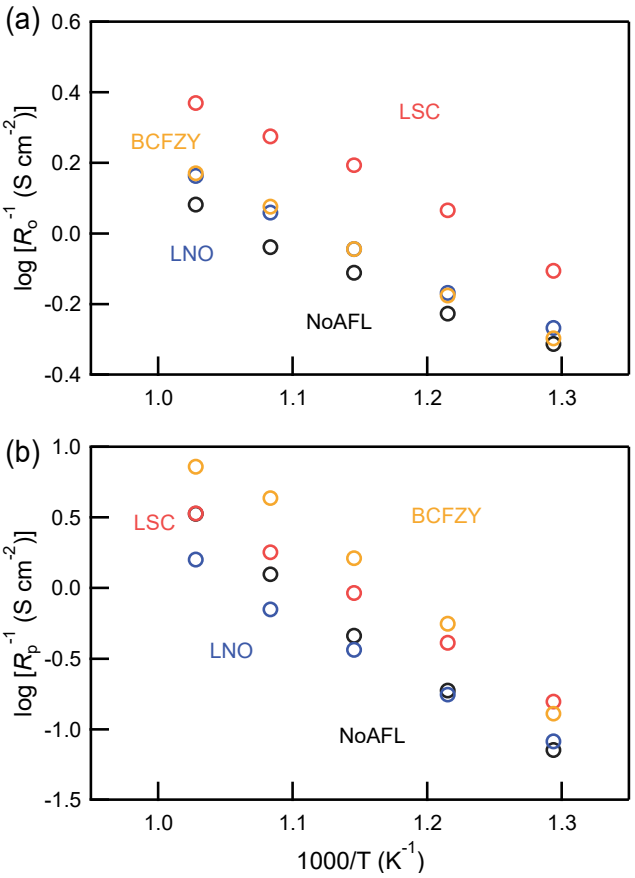

Fig. S9. Arrhenius plots of (a) ohmic resistance (R_o) and (b) anodic polarization resistance (R_p) as determined by equivalent circuit analysis using EIS for NoAFL LNO, LSC and BCFZY cell.

Table S2 Comparison of activation energies of ohmic resistance (R_o) and anodic polarization resistance (R_p) for P-SOECs without and with different AFLs.

Anode functional layer (AFL)	Activation energy for R_o	Activation energy for R_p
NoAFL	0.29	1.24
LSC4	0.31	1.04
PBSCF	0.32	1.01
BLFZ	0.24	0.78
BPY	0.31	1.17
LNO	0.32	0.95
LSC	0.35	0.99
BCFZY	0.36	1.32

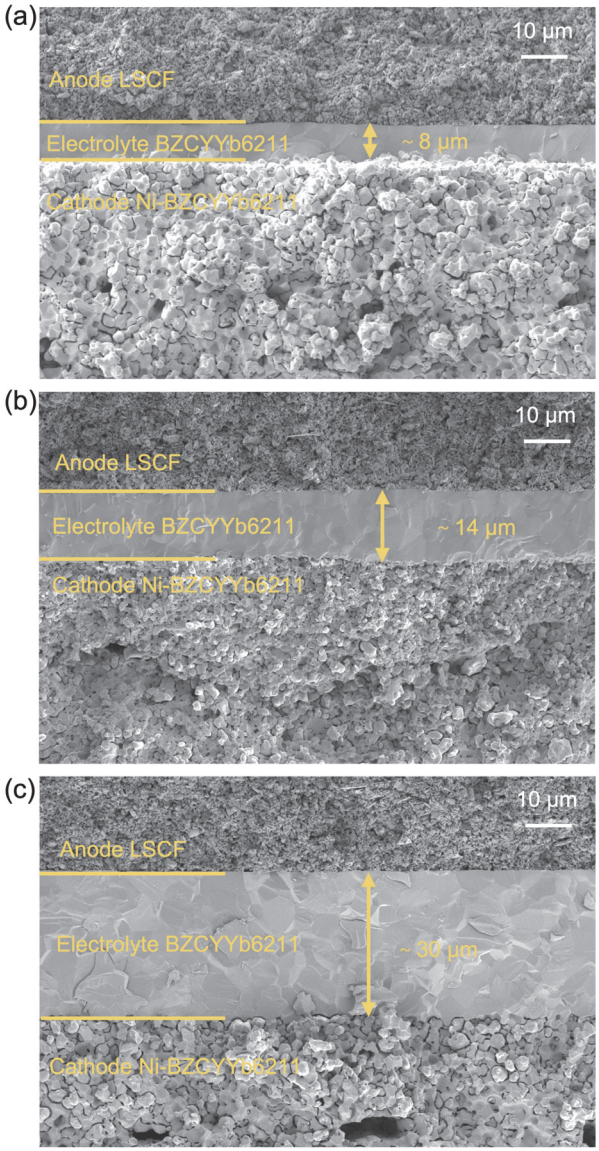

Fig. S10. Cross-sectional SEM images of NoAFL cells with different thicknesses of BZCYYb6211 electrolyte.

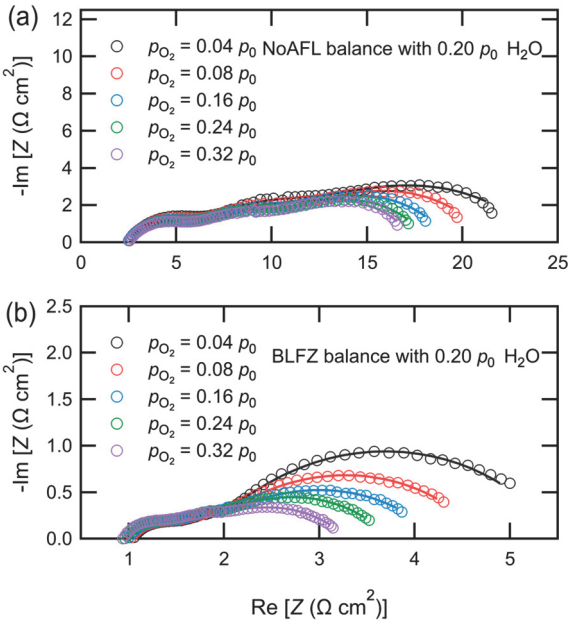

Fig. S11. EIS of P-SOECs measured at 500 °C of (a) NoAFL and (b) BLFZ AFL cells as a function of oxygen partial pressures (p_{O_2}).

References:

1. F. He, D. Song, R. Peng, G. Meng and S. Yang, *J. Power Sources*, 2010, **195**, 3359–3364.
2. M. A. Azimova and S. McIntosh, *Solid State Ionics*, 2011, **203**, 57–61.
3. L. Bi, S. P. Shafi and E. Traversa, *J. Mater. Chem. A*, 2015, **3**, 5815–5819.
4. D. Huan, N. Shi, L. Zhang, W. Tan, Y. Xie, W. Wang, C. Xia, R. Peng and Y. Lu, *ACS Appl. Mater. Interfaces*, 2018, **10**, 1761–1770.
5. J. Lyagaeva, N. Danilov, G. Vdovin, J. Bu, D. Medvedev, A. Demin and P. Tsiakaras, *J. Mate. Chem. A*, 2016, **4**, 15390–15399.
6. L. Lei, Z. Tao, X. Wang, J. P. Lemmon and F. Chen, *J. Mater. Chem. A*, 2017, **5**, 22945–22951.
7. L. Lei, J. Zhang, R. Guan, J. Liu, F. Chen and Z. Tao, *Energy Conver. Manag.*, 2020, **218**, 113044.
8. D. Huan, W. Wang, Y. Xie, N. Shi, Y. Wan, C. Xia, R. Peng and Y. Lu, *J. Mater. Chem. A*, 2018, **6**, 18508–18517.
9. S. Yang, Y. Wen, J. Zhang, Y. Lu, X. Ye and Z. Wen, *Electrochim. Acta*, 2018, **267**, 269–277.
10. S. Yang, S. Zhang, C. Sun, X. Ye and Z. Wen, *ACS Appl. Mater. Interfaces*, 2018, **10**, 42387–42396.
11. W. Li, B. Guan, L. Ma, S. Hu, N. Zhang and X. Liu, *J. Mater. Chem. A*, 2018, **6**, 18057–18066.
12. W. Wu, D. Ding and T. He, *ECS Trans.*, 2017, **80**, 167–173.
13. Y. Meng, J. Gao, H. Huang, M. Zou, J. Duffy, J. Tong and K. S. Brinkman, *J. Power Sources*, 2019, **439**, 227093.
14. Y. Song, J. Liu, Y. Wang, D. Guan, A. Seong, M. Liang, M. J. Robson, X. Xiong, Z. Zhang, G. Kim, Z. Shao and F. Ciucci, *Adv. Energy Mater.*, 2021, **11**, 2101899.